

# Discrete Abelian lattice gauge theories on a ladder and their dualities with quantum clock models

S. Pradhan,<sup>1,2,\*</sup> A. Maroncelli,<sup>3,4,\*</sup> and E. Ercolessi<sup>1,2</sup>

<sup>1</sup>*Dipartimento di Fisica e Astronomia, Università di Bologna, 40127 Bologna, Italy*

<sup>2</sup>*INFN, Sezione di Bologna, I-40127 Bologna, Italy*

<sup>3</sup>*Dipartimento di Fisica e Astronomia, Università di Firenze, 50019 Firenze, Italy*

<sup>4</sup>*INFN, Sezione di Firenze, I-50019 Firenze, Italy*

We study a duality transformation from the gauge-invariant subspace of a  $\mathbb{Z}_N$  lattice gauge theory on a two-leg ladder geometry to an  $N$ -clock model on a single chain. The main feature of this mapping is the emergence of a longitudinal field in the clock model, whose value depends on the superselection sector of the gauge model, implying that the different sectors of the gauge theory can show quite different phase diagrams. In order to investigate this and see if confined phases might emerge, we perform a numerical analysis for  $N = 2, 3, 4$ , using exact diagonalization.

Gauge theories constitute the baseline in our microscopical description of physical fundamental laws and are a cornerstone of contemporary scientific research. Calculations beyond perturbative regimes, as needed to understand for example the quark confinement mechanism in quantum chromodynamics, represent a notorious challenge both analytically and numerically. Standard classical computational methods adopt the Wilson's framework of lattice gauge theories (LGTs) [1–3], in which the continuous space–time is replaced by a discrete set of points and the calculations are performed in the Euclidean path-integral approach. More recently, inspired by idea by Feynman about quantum simulations [4, 5], many authors have adopted a Hamiltonian approach in which only spatial coordinates are discretized, and which might be implemented via a quantum platform once the group degrees of freedom are also discretized, by considering a finite group or by suitable approximations (see [6–10] and references therein). Still, in all approaches, enforcing the gauge constraints to restrict the (analytical, numerical or experimental) evaluation of observables to the gauge-invariant Hilbert subspace is a challenging task, which is dealt with different strategies.

In this paper we consider Abelian LGTs, which are known to exhibit confined/deconfined phases [11–19]. More specifically, we introduce a pure  $\mathbb{Z}_N$  gauge model on a (quasi-2D) ladder geometry, which includes both electric and magnetic degrees of freedom and admits superselection sectors, similarly to what happens in the Toric code. To tackle the problem of gauge invariance, we make use of a bond algebraic approach [20, 21] to introduce a duality transformation that allows for an exact mapping from the LGT on the ladder restricted to the gauge-invariant Hilbert space to a 1D  $N$ -clock model [22–26] with a transversal field and a longitudinal field. The value of the latter turns out to depend on the superselection sector of the ladder LGT, resulting in possible different phase diagrams for the different sectors. To see this, we use exact diagonalization to calculate Wilson loops and study the appearance of confined phases.

**The lattice gauge model.** Following the Hamiltonian approach of Kogut and Susskind [2], we consider a class of pure Abelian lattice gauge theories, with  $\mathbb{Z}_N$  gauge group, on a *ladder geometry*, which consists of a lattice  $\mathbb{L}$  made of two parallel chains, the *legs*, coupled to each other by *rungs* to form square plaquettes. On the ladder, each rung is identified by a coordinate  $i = 1, \dots, L$ , where  $L$  is the length of the ladder, and the two vertices on the rung are denoted with  $i^\uparrow$  and  $i^\downarrow$  in the upper and lower leg, respectively. Links are denoted by  $\ell$ . On the legs they are labelled as  $\ell_i^\uparrow$  (upper leg) or  $\ell_i^\downarrow$  (lower leg), while those on the rungs are labelled  $\ell_i^0$ .

The gauge group degrees of freedom are defined on the links. For a finite group like  $\mathbb{Z}_N$ , the notion of infinitesimal generators loses any meaning and we are led to directly consider, for each link  $\ell \in \mathbb{L}$ , a pair of conjugate operators,  $U_\ell$  and  $V_\ell$  which are unitary and defined by the algebraic relations [27–29]

$$V_\ell U_\ell = \omega U_\ell V_\ell, \quad U_\ell^N = V_\ell^N = \mathbb{1}_N \quad (1)$$

with  $\omega = e^{i(\frac{2\pi}{N} + \phi)}$ , where the angle  $\phi$  is arbitrary and corresponds to the physical situation in which on each link there is a background electric field [29, 30]. In this letter we don't consider this situation and will set  $\phi = 0$ . Also, these operators commute on different links. This algebra admits a faithful finite-dimensional representation of dimension  $N$  [28, 31]. To each link  $\ell$ , we associate an  $N$ -dimensional Hilbert space  $\mathcal{H}_\ell$  generated by an orthonormal basis  $\{|v_{k,\ell}\rangle\}$ , with  $k = 0, \dots, N-1$ , the *electric basis*, that diagonalizes  $V_\ell$ , with:  $V_\ell |v_{k,\ell}\rangle = \omega_\ell^k |v_{k,\ell}\rangle$ . On this basis,  $U_\ell$  acts as a shift operator, i.e.  $U_\ell |v_{k,\ell}\rangle = |v_{k+1,\ell}\rangle$ , where  $k+1$  is taken mod  $N$ .

As shown in the top panel of Fig. 1, we use the symbols  $V_i^0$ ,  $U_i^0$  for the operators defined on the rung  $i$ , and  $V_i^\rho$ ,  $U_i^\rho$  with  $\rho = \uparrow, \downarrow$  for the operators on the horizontal links of the upper and lower leg to the right of the rung. The links on the legs are oriented from left to right while those on the rungs from bottom to top. To construct a LGT, in addition to the *electric field operators*  $V$ 's defined above, we need:

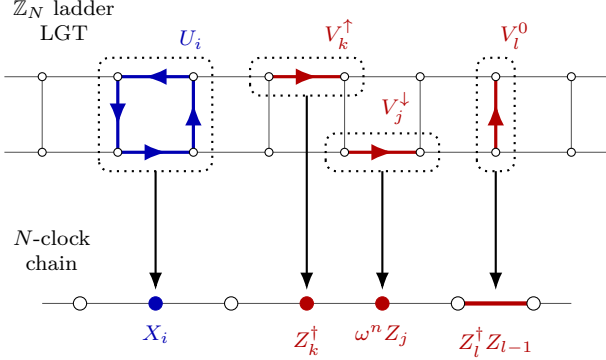


FIG. 1. Visual representation of local operators of the  $\mathbb{Z}_N$  ladder LGT and the duality transformation to the  $N$ -clock model.

- the *magnetic operators*, which are defined on each plaquette to the right of the rung  $i$  via the formula:

$$U_i = U_i^\downarrow U_{i+1}^0 (U_i^\uparrow)^\dagger (U_i^0)^\dagger; \quad (2)$$

- the *Gauss operators*, which are defined on each vertex  $i^\uparrow, i^\downarrow$  of the lattice as:

$$G_i^\uparrow = V_i^\uparrow (V_{i-1}^\uparrow)^\dagger (V_i^0)^\dagger, \quad G_i^\downarrow = V_i^\downarrow V_i^0 (V_{i-1}^\downarrow)^\dagger \quad (3)$$

and implement local gauge transformations, by imposing that physical states should satisfy:  $G_i^\rho |\Psi_{\text{phys}}\rangle = |\Psi_{\text{phys}}\rangle$  for  $\rho = \uparrow, \downarrow$  and  $\forall i$ .

It is simple to verify that the  $U_i$ -operators commute with all Gauss operators, making them gauge invariant.

The gauge-invariant Hamiltonian we use to build a  $\mathbb{Z}_N$  LGT on the ladder can be written as:

$$H_{\mathbb{Z}_N} = - \sum_i \left[ U_i + \lambda \left( V_i^\uparrow + V_i^\downarrow + V_i^0 \right) + \text{h.c.} \right], \quad (4)$$

with  $\lambda > 0$ . We use periodic boundary conditions on legs.

Similarly to what happens in the two dimensional Toric Code [13, 32], the Hilbert space of physical states  $\mathcal{H}_{\text{phys}}$  can be decomposed as a direct sum of superselection sectors  $\mathcal{H}_{\text{phys}}^{(n)}$ , where  $n = 0, \dots, N-1$ , that can be distinguished by means of the operators

$$\bar{S} = V_{i_0}^\uparrow V_{i_0}^\downarrow, \quad \bar{W} = \prod_{i \in \mathcal{C}_0} U_i^\downarrow, \quad (5)$$

where  $i_0$  labels the position of an arbitrary rung in the lattice, while  $\mathcal{C}_0$  is any non-contractible loop around the ladder. They satisfy the relations:  $\bar{W} \bar{S} = \omega \bar{S} \bar{W}$ . Each physical state in a sector  $\mathcal{H}_{\text{phys}}^{(n)}$  is an eigenstate of  $\bar{S}$  with eigenvalue  $\omega^n$ , while  $\bar{W}$  maps  $\mathcal{H}_{\text{phys}}^{(n)}$  into  $\mathcal{H}_{\text{phys}}^{(n+1)}$  (see [33]).

**Duality transformation to clock models.** Clock models [22–24] are a class of models that can be thought

as a generalization of the quantum Ising model. A  $p$ -state clock model on a chain has a local  $p$ -dimensional Hilbert space for each site  $i = 1, \dots, L$  and employs  $p \times p$  unitary matrices  $X_i$  and  $Z_i$  that commute on different sites, while on the same site

$$X_i Z_i = \omega Z_i X_i, \quad (X_i)^p = (Z_i)^p = \mathbb{1}_p, \quad (6)$$

with  $\omega = e^{i2\pi/p}$ . For example, one can choose a basis where the  $Z_i$ s are diagonal, i.e.  $(Z_i)_{mn} = \delta_{m,n} \omega^m$  and  $(X)_{mn} = \delta_{m,n+1} \pmod{p}$ , with  $m, n = 0, \dots, p-1$ . The  $p$ -clock Hamiltonian is given by

$$H_p(h) = - \sum_i \left( Z_{i-1}^\dagger Z_i + h X_i + \text{h.c.} \right), \quad (7)$$

where periodic boundary conditions are assumed.

We use the bond-algebraic approach to dualities [20], to introduce a *gauge reducing duality* mapping between the  $\mathbb{Z}_N$  gauge model (with redundant degrees of freedom) on the ladder and an  $N$ -clock model on a single chain. As a first step, similarly to what it can be done in 2D [3, 20, 34], we associate to each plaquette of the LGT a site of the chain of the clock model, in such a way that the gauge-invariant magnetic operator  $U_i$  is mapped into the single-body operator  $X_i$ . Also, since the electric field on a rung link  $\ell_i^0$  is the result of the flux difference between the two adjacent plaquettes, we map the operator  $V_i^0$  to a kinetic-type term of the kind  $Z_{i-1}^\dagger Z_i$ . As a second step, we consider the ladder operators  $V_i^\uparrow$  and  $V_i^\downarrow$  that explicitly enter the definition of the Gauss law operators of (3) and the  $\bar{S}$  operators of (5). We define the mapping to clock-operators via:  $V_i^\downarrow \mapsto \alpha_i^\uparrow Z_i$ ,  $V_i^\uparrow \mapsto \alpha_i^\downarrow Z_i^\dagger$ , where the complex coefficients  $\alpha_i^\uparrow, \alpha_i^\downarrow$  have to be chosen so that:

- i) the algebra commutation relations (1) are preserved;
- ii) Gauss law is automatically enforced, i.e.  $G_i^\uparrow, G_i^\downarrow \mapsto \mathbb{1}$ ;
- iii) in each superselection sector we have  $\bar{S} \mapsto \omega^n \mathbb{1}$ .

These requirements lead to the following *sector-dependent duality map* (see [33]):

$$\begin{aligned} U_i &\mapsto X_i, & V_i^0 &\mapsto Z_{i-1}^\dagger Z_i, \\ V_i^\uparrow &\mapsto Z_i^\dagger, & V_i^\downarrow &\mapsto \omega^n Z_i. \end{aligned} \quad (8)$$

that transforms the Hamiltonian (4) into  $\lambda H_N$ , where  $H_N$  is

$$H_N = H_p(1/\lambda) - \left[ (1 + \omega^n) \sum_i Z_i + \text{h.c.} \right]. \quad (9)$$

The novelty of (9) is the appearance of a *longitudinal field* term, with a coupling  $(1 + \omega^n)$  that depends explicitly on the superselection sector  $n$ . Notice that when  $N$  is even, the longitudinal field is zero for  $n = N/2$ . This simple fact makes it reasonable to think that different superselection sectors of the same ladder model can have drastically different phase diagrams.

Let us remark that the complex coupling  $(1 + \omega^n)$  does not make the Hamiltonian (9) necessarily chiral [35, 36]. In fact, one can get the real Hamiltonian

$$H_N = H_p(1/\lambda) - 2 \cos\left(\frac{\pi n}{N}\right) \sum_i (Z_i + Z_i^\dagger). \quad (10)$$

by absorbing the complex phase in the  $Z_i$ -operators, with the transformation  $Z_i \mapsto \omega^{-n/2} Z_i$ . This transformation globally rotates the eigenvalues of the  $Z_i$ -operators, while preserving the algebra relations. For  $n$  even, this is just a permutation of the eigenvalues, meaning that it does not affect the Hamiltonian spectrum. Instead, for  $n$  odd, up to a reorder, the eigenvalues are shifted by an angle  $\pi/N$ , i.e. half the phase of  $\omega$ . The energy contribution of the extra term in (10) depends on the real part of these eigenvalues and for  $n$  odd we obtain that the lowest energy state is no longer unique, in fact it is doubly degenerate. This means that for  $\lambda \rightarrow \infty$ , where the extra term becomes dominant, we expect an ordered phase with a doubly degenerate ground state. Finally, one can easily prove that the sectors  $n$  and  $N - n$  are equivalent [37].

**Numerical investigations.** We wish to investigate the presence of a *deconfined-confined phase transition* (DCPT) for a given  $\mathbb{Z}_N$  ladder LGT. In a pure gauge theory, these phases can be detected with the perimeter/area law for Wilson loops [1], which can be expressed as the products of magnetic operators over a given region. Unfortunately, in a ladder geometry there is not much difference between the area and the perimeter of a loop, since they both grow linearly in the size system  $L$ .

Nonetheless, we expect a phase transition by varying  $\lambda$  [13, 15, 16] that can still be captured by an operator like  $W_{\mathcal{R}} = \prod_{i \in \mathcal{R}} U_i$ , the product of magnetic operators  $U$ 's over a (connected) region  $\mathcal{R}$ . Indeed, when  $\lambda = 0$ , the Hamiltonian (4) is analogous to a Toric Code [32] which is known to be in a deconfined phase, where the (topologically distinct) ground states are obtained as uniform superpositions of the gauge-invariant states, i.e. closed electric loops. On these ground states  $\langle W_{\mathcal{R}} \rangle = 1$ , hence a value  $\langle W_{\mathcal{R}} \rangle \approx 1$  signals a deconfined phase. On the other hand, when  $\lambda \rightarrow \infty$ , the electric loops are suppressed, hence  $\langle W_{\mathcal{R}} \rangle \approx 0$ , signalling a confined phase.

In the dual clock model picture, the Wilson loop translates to a disorder operator [34], which means that a deconfined phase can be thought of as a paramagnetic (or disordered) phase, while the confined phase is like a ferromagnetic (or ordered) phase. Moreover, the longitudinal field breaks the  $N$ -fold symmetry of the ferromagnetic phase into a one-fold or two-fold degeneracy, depending on the parity ( $n$  even/odd) of the superselection sector.

We study the  $\mathbb{Z}_N$  LGT on a ladder numerically through *exact diagonalization*, by evaluating the half-ladder Wilson loop, i.e.

$$W = U_1 U_2 \cdots U_{L/2}, \quad (11)$$

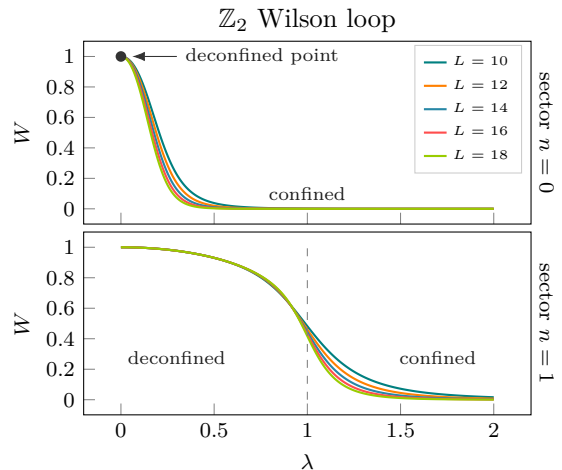


FIG. 2. Half-ladder Wilson loop for the  $\mathbb{Z}_2$  LGT in the sectors  $n = 0$  (top) and  $n = 1$  (bottom), for different lattice sizes (for length  $L = 10$  to  $L = 18$ ). The sector  $n = 0$  presents only a deconfined point at  $\lambda = 0$  and then decays rapidly into a confined phase, while the sector  $n = 1$  has a phase transition for  $\lambda \simeq 1$ .

and working in the restricted physical Hilbert space  $\mathcal{H}_{\text{phys}}^{(n)}$  ( $n = 0, \dots, N-1$ ), which has dimension  $N^L$ , much smaller than  $N^{3L}$  (the dimension of the total Hilbert space).

The naive and brute-force method for building  $\mathcal{H}_{\text{phys}}$  would require checking the Gauss law at every site (which are  $O(3L)$  operations) for all the possible  $N^{3L}$  candidate states. On the other hand, the gauge-reducing duality to clock models provides a faithful and efficient method for building the  $N^{L+1}$  basis states of  $\mathcal{H}_{\text{phys}}$ , yielding a major speedup with respect to the naive method (see [33]). The procedure is quite simple and it consists in treating a clock state as a plaquette flux state in the following way. Let  $|\Omega_0\rangle$  be the vacuum state where all the links are in the  $|0\rangle$  state. For each sector  $n$  we can build a “vacuum” state  $|\Omega_n\rangle$  by applying  $\bar{W}$  in (5)  $n$  times on the true vacuum, i.e.  $|\Omega_n\rangle = \bar{W}^n |\Omega_0\rangle$ . Then, let  $|s_1 s_2 \cdots\rangle$  be a configuration of the dual  $N$ -clock model, where  $s_i = 0, \dots, N-1$ . Now, the equivalent ladder state in the  $n$ -th sector can be obtained with  $\prod_i U_i^{s_i} |\Omega_n\rangle$ .

In the following, we present the results with  $N = 2, 3$  and 4, for different lengths.

**Results for  $N = 2$ .** As a warm up, we consider the  $\mathbb{Z}_2$  ladder LGT, with lengths  $L = 10, 12, \dots, 18$ . This model is equivalent to a  $p = 2$  clock model, which is just the quantum Ising chain, with only two superselection sectors for  $n = 0$  and  $n = 1$ . When  $n = 1$ , the Hamiltonian contains only the transverse field and is integrable [38]. Thus, we expect a critical point for  $\lambda \simeq 1$ , which will be a DCPT in the gauge model language. This is clearly seen in the behaviour of the half-ladder Wilson loop, as shown in the lower panel of Fig. 2. For  $n = 0$ , both the transverse and longitudinal fields are present,

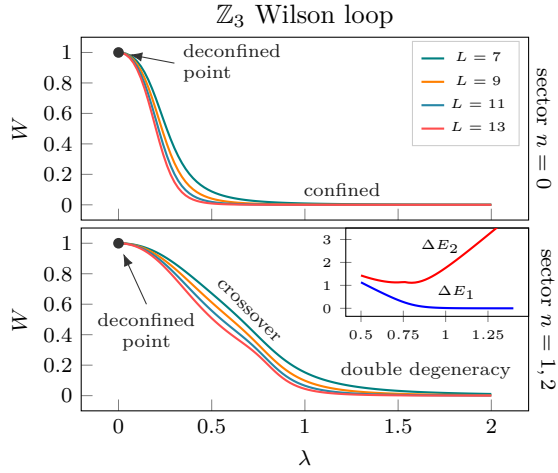


FIG. 3. Half-ladder Wilson loop values for  $\mathbb{Z}_3$  LGT for the sectors  $n = 0$  (top) and the two equivalent ones  $n = 1, 2$  (bottom), for sizes  $L = 7, 9, 11$  and  $13$ .

Inset: energy differences  $\Delta E_i = E_i - E_0$  for  $i = 1, 2$ , as a function of the coupling  $\lambda$ , in the sectors  $n = 1, 2$ , showing the emergence of a double-degenerate ground state for  $\lambda > 1$ .

the model is no longer integrable [39–41] and we expect to always see a confined phase, except for  $\lambda = 0$ . This is indeed confirmed by the behaviour of the half-ladder Wilson loop shown in the upper panel of Fig. 2.

We can further characterize the phases of the two sectors by looking at the structure of the ground state, for  $\lambda < 1$  and  $\lambda > 1$ , which is possible thanks to the exact diagonalization. In particular, in the deconfined phase of the sector  $n = 1$ , the ground state is a superposition of the deformations of the non-contractible electric string that makes the  $n = 1$  vacuum  $|\Omega_1\rangle$ . For this reason, this phase can be thought as a *kink condensate* [34] (which is equivalent to a paramagnetic phase), where each kink corresponds to a deformation of the string. Instead, for  $\lambda > 1$ , where we have confinement (as in the  $n = 0$  sector), the ground state is essentially a product state, akin to a ferromagnetic state (see [33]).

**Results for  $N = 3$ .** The  $\mathbb{Z}_3$  LGT is studied for lengths  $L = 7, 9, 11$  and  $13$ . This model can be mapped to a 3-clock model, which is equivalent to a 3-state quantum Potts model with a longitudinal field, which is present in all sectors, as one can see from (10). This field is expected to disrupt any ordered state and thus it is not possible to observe a phase transition, as it is confirmed by the behaviour of the half-ladder Wilson loops shown in Fig. 3. In addition, all the sectors present a deconfined point at  $\lambda = 0$ . In the case  $n = 0$ , for  $\lambda > 0$  we recognize a quick transition to a confined phase, similar to what happens in [19]. While for  $n = 1$  and  $2$  (which are equivalent), the model exhibits a smoother *crossover* to an ordered phase characterized by a doubly-degenerate ground state, for  $\lambda > 1$ . Notice that, as discussed above, the presence of the “skew” longitudinal field breaks the

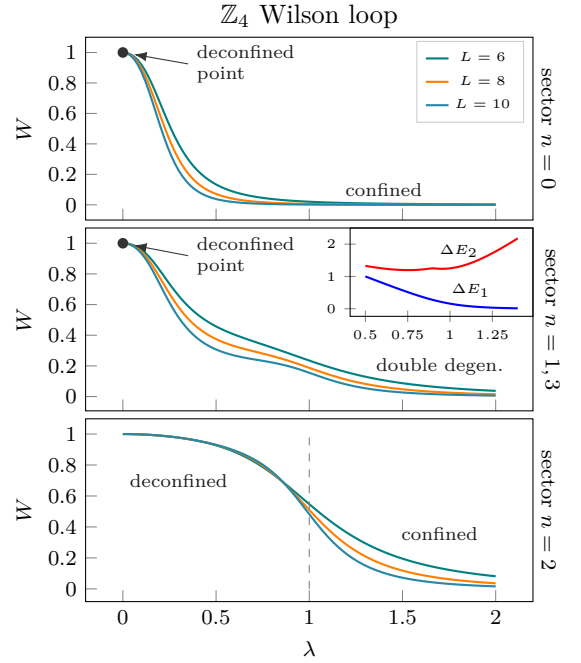


FIG. 4. Half-ladder Wilson loop values for the  $\mathbb{Z}_4$  LGT for all the sectors ( $n = 0, \dots, 3$ ) and different sizes ( $L = 6, \dots, 10$ ). Only the sector  $n = 2$  has a clear deconfined-confined phase transition, as expected from the duality with the 4-clock model.

three-fold degeneracy expected in the ordered phase of the 3-clock model into a two-fold degeneracy only.

**Results for  $N = 4$ .** The  $\mathbb{Z}_4$  ladder LGT has four superselection sectors. The behaviour of half-ladder Wilson loops as function of  $\lambda$  is shown in Fig. 4. As in the previous models, for  $n = 0$  we see a deconfined point at  $\lambda = 0$ , followed by a sharp transition to a confined phase. The sector  $n = 2$ , which has no longitudinal field, is the only one to present a clear DCPT for  $\lambda \approx 1$ , as it is expected from the fact that the 4-clock model is equivalent to two decoupled Ising chains [23]. In the two equivalent sectors  $n = 1$  and  $3$ , where the longitudinal field is complex, the Wilson loop shows a peculiar behaviour, at least for the largest size ( $L = 10$ ) of the chain: it decreases fast as soon  $\lambda > 0$ , to stabilize to a finite value in the region  $0.5 \lesssim \lambda \lesssim 1$ , before tending to zero. The characteristics of this phase would deserve a deeper analysis, that we plan to do in a future work. For  $\lambda \gtrsim 1$ , the system enters a deconfined phase with a double degenerate ground state, as for the  $\mathbb{Z}_3$  model.

**Conclusions and outlooks.** In this work, we proposed an exact gauge preserving duality transformation that maps the  $\mathbb{Z}_N$  lattice gauge theory on a ladder onto a 1D  $N$ -clock model in a transversal field, coupled to a possibly complex longitudinal field which depends on the superselection sector.

This map allowed us to perform numerical simulations with an exact diagonalization algorithm with sizes up to



$L = 18, 13, 10$  for  $N = 2, 3, 4$  respectively. To study the phases of the model and a possible DCPT transition, we calculated the Wilson loops in the different topological sectors, finding an unusual behaviour in the sectors with  $n$  odd (mod  $N$ ), possibly suggesting the emergence of a new phase, such as for example the incommensurate phase appearing in chiral clock models [25, 36, 42], whose characterization requires however to consider longer sizes of the chain in order to evaluate the asymptotic behaviour of correlators. This will be the subject of future work, in which we can also consider the possibility to include static and dynamical matter in the lattice gauge model.

**Acknowledgments.** Numerical simulations have been performed with the QuSpin library for exact diagonalization [43, 44]. We thank M. Burrello and O. Pomponio for useful discussions. This research is partially supported by INFN through the project “QUANTUM”, the project “SFT” and the project “QuantHEP” of the QuantERA ERA-NET Co-fund in Quantum Technologies (GA No. 731473).

---

\* These authors have contributed equally.

- [1] K. G. Wilson, *Phys. Rev. D* **10**, 2445 (1974).
- [2] J. Kogut and L. Susskind, *Phys. Rev. D* **11**, 395 (1975).
- [3] J. B. Kogut, *Rev. Mod. Phys.* **51**, 659 (1979).
- [4] R. P. Feynman, in *Feynman and computation* (CRC Press, 2018) pp. 133–153.
- [5] R. P. Feynman, *Optics News* **11**, 11 (1985).
- [6] M. C. Bañuls, R. Blatt, J. Catani, A. Celi, J. I. Cirac, M. Dalmonte, L. Fallani, K. Jansen, M. Lewenstein, S. Montangero, *et al.*, *The European Physical Journal D* **74**, 1 (2020).
- [7] E. Zohar, J. I. Cirac, and B. Reznik, *Reports on Progress in Physics* **79**, 014401 (2015).
- [8] M. Dalmonte and S. Montangero, *Contemporary Physics* **57**, 388 (2016).
- [9] E. Zohar and M. Burrello, *Phys. Rev. D* **91**, 054506 (2015).
- [10] E. Zohar, A. Farace, B. Reznik, and J. I. Cirac, *Phys. Rev. A* **95**, 023604 (2017).
- [11] E. Fradkin and S. H. Shenker, *Phys. Rev. D* **19**, 3682 (1979).
- [12] D. Horn, M. Weinstein, and S. Yankielowicz, *Phys. Rev. D* **19**, 3715 (1979).
- [13] L. Tagliacozzo and G. Vidal, *Phys. Rev. B* **83**, 115127 (2011).
- [14] L. Tagliacozzo, A. Celi, A. Zamora, and M. Lewenstein, *Annals of Physics* **330**, 160 (2013).
- [15] A. Hama and D. A. Lidar, *Phys. Rev. Lett.* **100**, 030502 (2008).
- [16] S. Trebst, P. Werner, M. Troyer, K. Shtengel, and C. Nayak, *Phys. Rev. Lett.* **98**, 070602 (2007).
- [17] P. Emonts, M. C. Bañuls, I. Cirac, and E. Zohar, *Phys. Rev. D* **102**, 074501 (2020).
- [18] E. Zohar, A. Farace, B. Reznik, and J. I. Cirac, *Phys. Rev. Lett.* **118**, 070501 (2017).
- [19] J. Nyhegn, C.-M. Chung, and M. Burrello, *Phys. Rev. Research* **3**, 013133 (2021).
- [20] E. Cobanera, G. Ortiz, and Z. Nussinov, *Advances in physics* **60**, 679 (2011).
- [21] Z. Nussinov and G. Ortiz, *Phys. Rev. B* **79**, 214440 (2009).
- [22] R. J. Baxter, *Physics Letters A* **140**, 155 (1989).
- [23] G. Ortiz, E. Cobanera, and Z. Nussinov, *Nuclear Physics B* **854**, 780 (2012).
- [24] P. Fendley, *Journal of Physics A: Mathematical and Theoretical* **47**, 075001 (2014).
- [25] Y. Zhuang, H. J. Changlani, N. M. Tubman, and T. L. Hughes, *Phys. Rev. B* **92**, 035154 (2015).
- [26] G. Sun, T. Vekua, E. Cobanera, and G. Ortiz, *Phys. Rev. B* **100**, 094428 (2019).
- [27] J. Schwinger, *Proceedings of the National Academy of Sciences* **46**, 570 (1960).
- [28] S. Notarnicola, E. Ercolessi, P. Facchi, G. Marmo, S. Pascazio, and F. V. Pepe, *Journal of Physics A: Mathematical and Theoretical* **48**, 30FT01 (2015).
- [29] E. Ercolessi, P. Facchi, G. Magnifico, S. Pascazio, and F. V. Pepe, *Phys. Rev. D* **98**, 074503 (2018).
- [30] G. Magnifico, M. Dalmonte, P. Facchi, S. Pascazio, F. V. Pepe, and E. Ercolessi, *Quantum* **4**, 281 (2020).
- [31] H. Weyl, *The theory of groups and quantum mechanics* (Courier Corporation, 1950).
- [32] A. Y. Kitaev, *Annals of Physics* **303**, 2 (2003).
- [33] See the Supplemental Materials for details about the state structure of the LGT, a review of the bond-algebraic approach to dualities, numerical implementation of Gauss law and physical states.
- [34] E. Fradkin and L. Susskind, *Phys. Rev. D* **17**, 2637 (1978).
- [35] P. Fendley, *Journal of Statistical Mechanics: Theory and Experiment* **2012**, P11020 (2012).
- [36] S. Whitsitt, R. Samajdar, and S. Sachdev, *Phys. Rev. B* **98**, 205118 (2018).
- [37] For the sector  $N - n$  we have that the overall factor  $\cos(\pi(N-n)/N)$  is just  $-\cos(\pi n/N)$ . The minus sign can then be again absorbed into the  $Z$ ’s operators. This overall operation is equivalent to the mapping  $Z \mapsto \omega^{-n/2} Z$  for the sector  $N - n$ .
- [38] R. J. Baxter, *Exactly solved models in statistical mechanics* (Elsevier, 2016).
- [39] M. C. Bañuls, J. I. Cirac, and M. B. Hastings, *Phys. Rev. Lett.* **106**, 050405 (2011).
- [40] M. Kormos, M. Collura, G. Takács, and P. Calabrese, *Nature Physics* **13**, 246 (2017).
- [41] O. Pomponio, M. A. Werner, G. Zarand, and G. Takacs, *SciPost Phys.* **12**, 61 (2022).
- [42] D. A. Huse, A. M. Szpilka, and M. E. Fisher, *Physica A: Statistical Mechanics and its Applications* **121**, 363 (1983).
- [43] P. Weinberg and M. Bukov, *SciPost Phys.* **2**, 003 (2017).
- [44] P. Weinberg and M. Bukov, *SciPost Phys.* **7**, 20 (2019).
- [45] J. Schwinger and B. Englert, “Symbolism of atomic measurements,” (2001).
- [46] H. A. Kramers and G. H. Wannier, *Phys. Rev.* **60**, 252 (1941).
- [47] D. Radicevic, “Spin structures and exact dualities in low dimensions,” (2019), [arXiv:1809.07757 \[hep-th\]](https://arxiv.org/abs/1809.07757).
- [48] Thanks to (S36) we also know how to treat static matter. Since it can be viewed as a violation of Gauss law, we just have to change the phases of  $c_i^\dagger$  and  $c_i^\dagger$ .

## Supplemental Materials to “Discrete Abelian lattice gauge theories on a ladder and their dualities with quantum clock models”

In order to understand the structure of the  $\mathbb{Z}_N$  lattice gauge model on a ladder geometry, we review here the definition and the properties of the analogous model in two dimensions, by also discussing the bond-algebraic approach to find a gauge-reducing duality transformation. We then adapt the latter to the ladder model, obtaining an  $N$ -clock model with both transversal and longitudinal field. Finally, we give some details on the results of the numerical analysis performed via exact diagonalization.

### I. REVIEW OF TWO-DIMENSIONAL LGTS AND THE TORIC CODE

In this section we review lattice gauge theories (LGT) on a two dimensional lattice and their connection to the Toric Code. To do so, we introduce the Schwinger-Weyl algebra and lattice gauge transformations.

According to Wilson’s Hamiltonian approach to lattice gauge theories [1],  $U(1)$  gauge fields are defined on the links of a lattice  $\mathbb{L}$  either in a pair of conjugate variables, the electric field  $E_\ell$  and either the vector potential  $A_\ell$ , satisfying  $[E_\ell, A_{\ell'}] = i\delta_{\ell,\ell'}$ , or equivalently the magnetic operator, also called comparator,  $U_\ell = e^{-iA_\ell}$ , such that  $[E_\ell, U_{\ell'}] = \delta_{\ell,\ell'} U_\ell$ , all acting on an infinite dimensional Hilbert space defined on each link. This form of the canonical commutation relations represents the infinitesimal version of the relations:  $e^{i\xi E} e^{-i\eta A} e^{-i\xi E} = e^{i\xi\eta} e^{-i\eta A}$ , for any  $\xi, \eta \in \mathbb{R}$ , that define the Schwinger-Weyl group [27–29].

For a discrete group like  $\mathbb{Z}_N$ , the notion of infinitesimal generators loses any meaning and we are led to directly consider, for each link  $\ell \in \mathbb{L}$ , two unitary operators  $V_\ell, U_\ell$ , such that [27, 45]

$$V_\ell U_\ell V_\ell^\dagger = e^{2\pi i/N} U_\ell, \quad U_\ell^N = \mathbb{1}_N, \quad V_\ell^N = \mathbb{1}_N. \quad (\text{S1})$$

while on different links they commute. Thus, by representing  $\mathbb{Z}_N$  with the set of the  $N$  roots of unity  $e^{i2\pi k/N}$  ( $k = 1, \dots, N$ ), commonly referred to as the discretized circle, we see that  $V$  plays the role of a “position operator” on the discretized circle, while  $U$  that of a “momentum operator”.

These algebraic relations admit a faithful finite-dimensional representation of dimension  $N$  [31], for any integer  $N$ , which is obtained as follows. To each link  $\ell$ , we can associate an  $N$ -dimensional Hilbert space  $\mathcal{H}_\ell$  generated by an orthonormal basis  $\{|v_{k,\ell}\rangle\}$  ( $k = 1, \dots, N$ ), called the *electric basis*, that diagonalizes  $V_\ell$ . With this choice, we can promptly write the actions of  $U_\ell$  and  $V_\ell$ :

$$\begin{aligned} U |v_{k,\ell}\rangle &= |v_{k+1,\ell}\rangle, & U |v_{N,\ell}\rangle &= |v_{1,\ell}\rangle \\ U^\dagger |v_{k,\ell}\rangle &= |v_{k-1,\ell}\rangle, & U^\dagger |v_{1,\ell}\rangle &= |v_{N,\ell}\rangle \\ V |v_{k,\ell}\rangle &= \omega^k |v_{k,\ell}\rangle, & V^\dagger |v_{k,\ell}\rangle &= \omega^{-k} |v_{k,\ell}\rangle, \end{aligned} \quad (\text{S2})$$

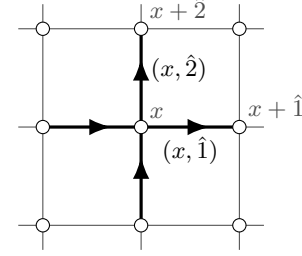


FIG. S1. Labelling of the sites and the links in the two dimensional lattice. A site is labeled simply with  $x = (x_1, x_2)$ , while  $\hat{1} = (1, 0)$  and  $\hat{2} = (0, 1)$  stand for the unit vectors of the lattice. A link  $\ell$  is denoted with a pair  $(x, \pm\hat{i})$ , with  $\hat{i} = \hat{1}, \hat{2}$ .

where  $\omega = e^{2\pi i/N}$  and  $k = 0, \dots, N-1$ . We choose to work in this particular basis and the various  $k$  can be interpreted as the quantized values of the electric field on the links.

On a two-dimensional square lattice of size  $L \times L$ , the links  $\ell$  of the lattice can also be labeled with  $(x, \pm\hat{i})$ , where  $x \in \mathbb{L}$  is a site and  $\hat{i} = \hat{1}, \hat{2}$  the two independent unit vectors. In this way,  $(x, \pm\hat{i})$  will refer to the link that starts in  $x$  and goes in the positive (negative) direction  $\hat{i}$  (see Fig. S1). This notation will be simplified when we reduce to the ladder case.

### Gauge invariance and physical states

Gauge transformations act on vector potentials while preserving the electric field. For a  $U(1)$  gauge theory, a local phase transformation is induced by a real function  $\alpha_x$  defined on the vertices  $x \in \mathbb{L}$ , such that  $A_\ell \rightarrow A_\ell + (\alpha_{x_2} - \alpha_{x_1})$  or equivalently  $U_\ell \rightarrow e^{i(\alpha_{x_2} - \alpha_{x_1})E_\ell} U_\ell e^{-i(\alpha_{x_2} - \alpha_{x_1})E_\ell}$ , where  $x_1, x_2$  are the initial and final vertices of the (directed) link  $\ell$ . In the case of a discrete symmetry, a gauge transformation at a site  $x \in \mathbb{L}$  is a product of  $V$ ’s (and  $V^\dagger$ ’s) defined on the links which comes out (and enters) the vertex. More specifically, for a two dimensional lattice, if the link  $\ell$  at site  $x$  is oriented in the positive direction, i.e. either  $(x, +\hat{1})$  or  $(x, +\hat{2})$ , then  $V$  is used, otherwise  $V^\dagger$ . Thus, the single local gauge transformation at the site  $x$  is enforced by

the operator:

$$G_x = V_{(x,\hat{1})} V_{(x,\hat{2})} V_{(x,-\hat{1})}^\dagger V_{(x,-\hat{2})}^\dagger, \quad (\text{S3})$$

as shown in the left part of in Fig. S2.

The whole operator algebra  $\mathcal{A}$  of the theory is generated by the set of all  $U_\ell$  and  $V_\ell$  (and their Hermitian conjugates) of all the links of the lattice  $\mathbb{L}$ , while the *gauge-invariant subalgebra*  $\mathcal{A}_{\text{gi}}$  consists of operators that commute with all the  $G_x$ :

$$\mathcal{A}_{\text{gi}} = \{O_{\text{gi}} \in \mathcal{A} : [O_{\text{gi}}, G_x] = 0 \quad \forall x \in \mathbb{L}\}. \quad (\text{S4})$$

Using (S3) and recalling (S1), it is possible to see that the  $V_\ell$ 's commute with  $G_x$  (as expected), while the  $U_\ell$ 's do not. In spite of that, we can build gauge-invariant operators out of the comparators  $U_\ell$ . Consider a *plaquette*  $\square$  of the lattice  $\mathbb{L}$  at  $x$ , by which we mean the face of the lattice with vertices  $\{x, x + \hat{1}, x + \hat{1} + \hat{2}, x + \hat{2}\}$  in the counterclockwise order, as shown in the right part of Fig. S2. On this plaquette, the operator  $U_\square$  is defined as

$$U_\square = U_{(x,\hat{1})} U_{(x+\hat{1},\hat{2})} U_{(x+\hat{1}+\hat{2},-\hat{1})}^\dagger U_{(x+\hat{2},-\hat{2})}^\dagger. \quad (\text{S5})$$

and one finds out that the  $U_\square$ 's commute with  $G_x$ , for all  $x \in \mathbb{L}$ , thus giving a generator of  $\mathcal{A}_{\text{gi}}$ .

The set  $\{U_\square, V_\ell\}$  (for all plaquettes  $\square$  and all links  $\ell$ ) may not be enough to generate the whole algebra  $\mathcal{A}_{\text{gi}}$ , in case of periodic boundary conditions. In order to prove this, consider a lattice  $\mathbb{L}$ , periodic in both dimensions, and denote with  $\mathcal{C}_1$  and  $\mathcal{C}_2$  any two *non-contractible loops* around the lattice, that extends along the  $\hat{1}$  and  $\hat{2}$  direction respectively. Then, define the (Wilson loop) operators  $\bar{W}_1$  and  $\bar{W}_2$  (pictured in blue in Fig. S3):

$$\bar{W}_i = \prod_{\ell \in \mathcal{C}_i} U_\ell, \quad i = 1, 2. \quad (\text{S6})$$

A simple calculation shows that both  $\bar{W}_1$  and  $\bar{W}_2$  commute with all  $G_x$ , thus they are gauge-invariant, but one also finds out that none of them can be written as a product of  $U_\square$  nor  $V_\ell$ . Therefore they have to be added explicitly to the set of generators of  $\mathcal{A}_{\text{gi}}$  in order to obtain the whole algebra. These operators  $\bar{W}_1$  and  $\bar{W}_2$  play a fundamental role in the model to define topological sectors of the theory, as we will see later.

The total Hilbert space  $\mathcal{H}^{\text{tot}}$  is given by the  $\otimes_\ell \mathcal{H}_\ell$ . A state of the whole lattice  $|\Psi_{\text{ph}}\rangle \in \mathcal{H}^{\text{tot}}$  is said to be *physical* if it is a *gauge-invariant state*:

$$G_x |\Psi_{\text{ph}}\rangle = |\Psi_{\text{ph}}\rangle, \quad \forall x \in \mathbb{L} \quad (\text{S7})$$

This condition can be translated into a constraint on the eigenvalues  $v_{(x,\pm\hat{i})} = \omega^{k_{(x,\pm\hat{i})}}$  of the operators  $V_\ell$  on the links  $\ell = (x, \pm\hat{i})$  of the vertex  $x$ :

$$v_{(x,\hat{1})} v_{(x,\hat{2})} v_{(x,-\hat{1})}^* v_{(x,-\hat{2})}^* = 1, \quad (\text{S8})$$

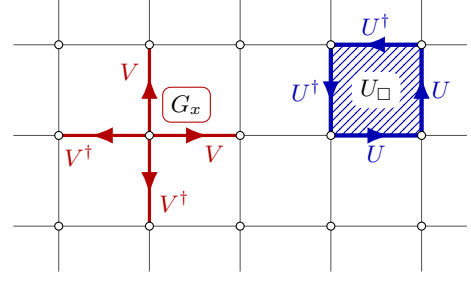


FIG. S2. Pictorial representation of the Gauss operators  $G_x$  in (S3) (left) and plaquette operator  $U_\square$  in (S5) (right).

or, because of (S2):

$$\sum_{i=1,2} \left( k_{(x,\hat{i})} - k_{(x,-\hat{i})} \right) = 0 \quad \text{mod } N. \quad (\text{S9})$$

Given the fact that the  $k$ 's in (S1) represent the values of the electric field, one can see that (S9) can be interpreted as a discretized version of the Gauss law  $\nabla \cdot \vec{E} = 0$  in two dimensions, for a pure gauge theory where there are no electric charges.

### $\mathbb{Z}_N$ Hamiltonian and the Toric Code

The class of models we consider are described by the Hamiltonian [13, 15, 16]:

$$H_{\mathbb{Z}_N}(\lambda) = - \sum_{\square} U_\square - \lambda \sum_{\ell} V_\ell + \text{h.c.}, \quad (\text{S10})$$

where the first sum is over the plaquettes  $\square$  of the lattice while the second sum is over the links  $\ell$ . One can easily see that this Hamiltonian is local and gauge-invariant, hence the dynamics it describes is fully contained in  $\mathcal{H}_{\text{phys}}$ . Furthermore, the operator  $U_\square$  plays the role of a *magnetic* term, to be more precise it is the magnetic flux inside the plaquette  $\square$ , while  $V$  is the *electric* term. The coupling  $\lambda$  tunes the relative strength of the electric and magnetic energy contribution.

These models are akin to the Toric Code [32], which can be thought as a prime example of a  $\mathbb{Z}_2$  lattice gauge theory. More precisely,  $H_{\mathbb{Z}_2}$  in (S10) can be thought as a *deformation* of the former, where an external “transverse” field is added to it. Indeed, using the notation used so far, the Toric Code can be formulated as:

$$H_{\text{TC}} = -J_m \sum_{\square} U_\square - J_e \sum_x G_x. \quad (\text{S11})$$

whose ground states  $|\Psi\rangle$  satisfy the constraints

$$U_\square |\Psi\rangle = |\Psi\rangle \quad \forall \square, \quad G_x |\Psi\rangle = |\Psi\rangle \quad \forall x. \quad (\text{S12})$$

Only elementary excitations above the ground state can violate these constraints and they can be of two type: a

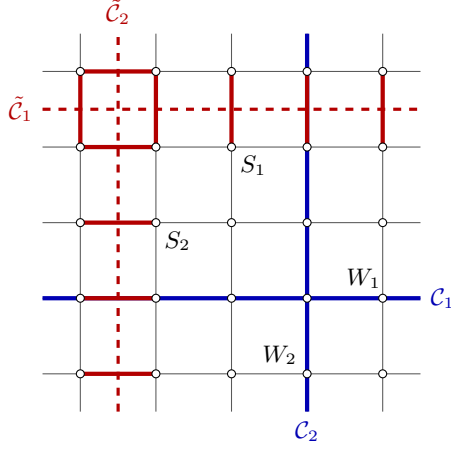


FIG. S3. Graphical representation of the non-local order parameters  $\bar{W}_{1,2}$  (in blue) and  $\bar{S}_{1,2}$  (in red) and their respective paths  $C_{1,2}$  and  $\tilde{C}_{1,2}$ .

*magnetic vortex* (which violates the plaquette constraint) or a *electric charge* (which violates the Gauss law). If one imposes  $J_e \gg J_m$  to enforce Gauss law, in the low-energy sector there are no electric charges and one recovers the pure gauge  $\mathbb{Z}_2$  model of (S10) for  $\lambda = 0$ . Therefore, in general the  $\mathbb{Z}_N$  models described in (S10) can be considered as generalization of the Toric Code, from the point of view of lattice gauge theories.

### Topological sectors

Let us consider the Toric Code. One of its main features is the presence of topologically protected degenerate ground states [32]. In order to illustrate this, besides  $\bar{W}_1$  and  $\bar{W}_2$ , defined in (S6), another type of non-local operators have to be introduced. They are defined on *cuts* of the lattice  $\mathbb{L}$ , i.e. paths on the dual lattice  $\tilde{\mathbb{L}}$ . Consider *non-contractible* cuts  $\tilde{C}_1$  and  $\tilde{C}_2$  along the directions  $\hat{1}$  and  $\hat{2}$ , respectively. On this cuts, the 't Hooft string) operators  $\bar{S}_1$  and  $\bar{S}_2$  are constructed as

$$\bar{S}_i = \prod_{\ell \in \tilde{C}_i} V_\ell, \quad i = 1, 2, \quad (\text{S13})$$

in a similar fashion to (S6). This is shown in red in Fig. S3. The operators  $\bar{W}_i$  and  $\bar{S}_i$  ( $i = 1, 2$ ) commutes with all the operators  $U_\square$  and  $G_x$  in the Toric Code Hamiltonian  $H_{\text{TC}}$  of (S11), but do not commute with each other. In fact, we have  $\bar{W}_i \bar{S}_j = -\bar{S}_j \bar{W}_i$  if  $i \neq j$ . This means that  $H_{\text{TC}}$  can be block-diagonalized with respect to the eigenvalues of  $\bar{S}_i$  (or  $\bar{W}_i$ ), while  $\bar{W}_j$  (or  $\bar{S}_j$ ) connects one block to the other. Furthermore, since in the case of the  $\mathbb{Z}_2$  symmetry,  $\bar{S}_i$  (or  $\bar{W}_i$ ) has only two eigenvalues (equal to  $\pm 1$ ), there are a total of  $2 \times 2 = 4$  degenerate ground states, which are topologically protected, thanks to the fact that  $\bar{W}_j$  (or  $\bar{S}_j$ ) cannot be

expressed in terms of the local operators  $U_\square$  and  $G_x$ . Notice that, as it can be easily seen, in the Toric Code the role of  $\bar{W}_i$  and  $\bar{S}_i$  can be interchanged.

Let us now turn to  $\mathbb{Z}_N$  LGT models. The operators  $\bar{W}_i$  no longer commute with the Hamiltonian (S10) which now contains an electric field term. Thus,  $\lambda \neq 0$ , we have no degenerate ground states. But we can still use the  $\bar{S}_i$  operators to decompose the Hilbert space  $\mathcal{H}_{\text{phys}}$ , since they still commute with all the *local operators*  $U_\square$  and  $V_\ell$  (thus also with  $H_{\mathbb{Z}_N}$ ). Now one can see that the operator  $\bar{S}_i$  ( $i = 1, 2$ ) of (S13) has  $N$  eigenvalues  $\omega^n$ , with  $n = 1, \dots, N-1$ . Hence, one can decompose  $\mathcal{H}_{\text{phys}}$  as sum of superselection sectors

$$\mathcal{H}_{\text{phys}} = \bigoplus_{n,m=0}^{N-1} \mathcal{H}_{\text{phys}}^{(n,m)}, \quad (\text{S14})$$

where for each  $|\phi\rangle \in \mathcal{H}_{\text{phys}}^{(n,m)}$  we have:

$$\bar{S}_1 |\phi\rangle = \omega^m |\phi\rangle, \quad \bar{S}_2 |\phi\rangle = \omega^n |\phi\rangle. \quad (\text{S15})$$

Let us consider now the role of the Wilson loops  $\bar{W}_i$ . One can easily see that:

$$\bar{W}_2 \bar{S}_1 = \omega \bar{S}_1 \bar{W}_2, \quad \bar{W}_1 \bar{S}_2 = \omega \bar{S}_2 \bar{W}_1. \quad (\text{S16})$$

It follows that  $\bar{W}_{1,2}$  acts a shift operators for the eigenspaces of  $\bar{S}_{2,1}$ :

$$\bar{W}_1 : \mathcal{H}_{\text{phys}}^{(n,m)} \rightarrow \mathcal{H}_{\text{phys}}^{(n+1,m)}, \quad \bar{W}_2 : \mathcal{H}_{\text{phys}}^{(n,m)} \rightarrow \mathcal{H}_{\text{phys}}^{(n,m+1)}, \quad (\text{S17})$$

where the integers  $n+1$  and  $m+1$  have to be taken mod  $N$ .

From a physical point of view, the Wilson loops operators  $\bar{W}_1$  and  $\bar{W}_2$  create non-contractible electric loops around the lattice, while the 't Hooft strings  $\bar{S}_2$  and  $\bar{S}_1$  detect the presence and the strength of these electric loops. Therefore, it is clear that the Hilbert subspace  $\mathcal{H}_{\text{phys}}^{(n,m)}$  is the subspace of all the states that contains an electric loop of strength  $\omega^n$  and  $\omega^m$  along the  $\hat{1}$  and  $\hat{2}$  direction, respectively. Furthermore, the evolution of a state in  $\mathcal{H}_{\text{phys}}^{(n,m)}$  with the Hamiltonian in (S10) is confined in  $\mathcal{H}_{\text{phys}}^{(n,m)}$ .

## II. REVIEW OF THE BOND-ALGEBRAIC APPROACH TO DUALITIES

In this section we review the bond-algebraic approach to dualities, because it offers a convenient way for dealing with duality transformations applied to gauge models. Details can be found in [20].

The concept of *bond-algebra* was introduced in [21] and it stems from the fact that most Hamiltonian are a sum of simple and (quasi)local terms:

$$H = \sum_{\Gamma} \lambda_{\Gamma} h_{\Gamma}, \quad (\text{S18})$$



where  $\Gamma$  is a set of indices (e.g. the lattice sites, as in the case we consider here) and  $\lambda_\Gamma$  are numbers. The terms  $h_\Gamma$  are called *bond operators* (or simply bonds) and they form a *bond algebra*  $\mathcal{A}\{h_\Gamma\}$ , which is the linear space of operators generated by all products of the bonds  $h_\Gamma$  and their Hermitian conjugates. The bonds  $h_\Gamma$  that generate  $\mathcal{A}\{h_\Gamma\}$  need not to be independent. Let us point out that a single Hamiltonian  $H$  can have different bond algebras associated to it, since the latter depend on how the total Hamiltonian  $H$  is partitioned into local terms.

In this framework, quantum dualities can be formulated as *homomorphisms of bond algebras*, i.e. structure preserving mappings between bond algebras. To be more precise, two Hamiltonians  $H_1$  and  $H_2$  that act on state spaces of the same dimension are said to be *dual* if there is some bond algebra  $\mathcal{A}_{H_1}$  of  $H_1$  that is homomorphic to some bond algebra  $\mathcal{A}_{H_2}$  of  $H_2$  and if the homomorphism  $\Phi : \mathcal{A}_{H_1} \rightarrow \mathcal{A}_{H_2}$  maps  $H_1$  onto  $H_2$ ,  $\Phi(H_1) = H_2$ . These mappings do not need to be isomorphisms, especially when gauge symmetries are involved, as we will explain below. Dualities, in this approach, are *local* with respect to the bonds, i.e. they map one bond  $h_{\Gamma_1}$  of  $H_1$  to one bond  $h_{\Gamma_2}$  of  $H_2$ , a fact that does not imply locality with respect to the elementary degrees of freedom, since the generators of a bond algebra are in general two (or more) body operators and a large (if not infinite) products of them is required to construct operators expressing elementary degrees of freedom.

To make this approach clearer we now apply it to the 1D quantum Ising model with transverse field. The Hamiltonian  $H_{\text{Ising}}$  is

$$H_{\text{Ising}}(\lambda) = \sum_i (\sigma_i^z \sigma_{i+1}^z + \lambda \sigma_i^x) \quad (\text{S19})$$

where  $\sigma_i^x$  and  $\sigma_i^z$  are the usual Pauli matrices for spin  $S = 1/2$ . We recognize as basic bonds the operators  $\{\sigma_i^x\}$  and  $\{\sigma_i^z \sigma_{i+1}^z\}$ . Their algebra relations can be summarized as follows:

- $(\sigma_i^x)^2 = \mathbb{1}$  and  $(\sigma_i^z \sigma_{i+1}^z)^2 = \mathbb{1}$
- for the bond  $\sigma_i^x$  we have that  $\{\sigma_i^x, \sigma_i^z \sigma_{i+1}^z\} = 0$  and  $\{\sigma_i^x, \sigma_{i-1}^z \sigma_i^z\} = 0$ , while it commutes with every other bond;
- for the bond  $\sigma_i^z \sigma_{i+1}^z$  we have that  $\{\sigma_i^z \sigma_{i+1}^z, \sigma_i^x\} = 0$  and  $\{\sigma_i^z \sigma_{i+1}^z, \sigma_{i+1}^x\} = 0$ , while it commutes with every other bond.

Let us define the mapping  $\Phi$  on the bonds as follows:

$$\Phi(\sigma_i^z \sigma_{i+1}^z) = \sigma_i^x, \quad \Phi(\sigma_i^x) = \sigma_{i-1}^z \sigma_i^z, \quad (\text{S20})$$

which easily extends to the full bond-algebra  $\mathcal{A}_{\text{Ising}}$ . It is clear that this map preserves all the important algebraic relationship and is one-to-one, hence it is an *isomorphism* of  $\mathcal{A}_{\text{Ising}}$  onto itself. The Hamiltonian  $H_{\text{Ising}}$  is just an

element of  $\mathcal{A}_{\text{Ising}}$  and through  $\Phi$  gets transformed to

$$\Phi(H_{\text{Ising}}(\lambda)) = \sum_i (\sigma_i^x + \lambda \sigma_i^z \sigma_{i+1}^z) = \lambda H_{\text{Ising}}(\lambda^{-1}), \quad (\text{S21})$$

yielding the standard duality transformation for the Ising model [34, 46].

A bond isomorphism on a bond algebra  $\mathcal{A}$  is physically sound if it is unitarily implementable [20], i.e. if there exists a unitary matrix  $\mathcal{U}$  such that

$$\Phi(\mathcal{O}) = \mathcal{U} \mathcal{O} \mathcal{U}^\dagger, \quad \forall \mathcal{O} \in \mathcal{A}, \quad (\text{S22})$$

a fact that we will assume from now on.

Let us now recall the notion of *gauge-reducing dualities*. The domain of such a map is a bond algebra of a model with gauge symmetries, i.e. a model with local constraints that signal the presence of redundant degrees of freedom. In this case, the space of states is larger than the set of physical states, which are invariant under the action of the local gauge operators. Also, a physical observable is represented by a gauge invariant Hermitian operator, i.e. an operator commuting with all local constraints. A gauge-reducing transformation trivially maps all local gauge operators to the identity, so its image is a “non-gauge” model.

In formulae, a gauge-reducing duality  $\Phi_{\text{GR}}$  has the properties:

$$\Phi_{\text{GR}}(H_{\text{G}}) = H_{\text{GR}}, \quad \Phi_{\text{GR}}(G_\Gamma) = \mathbb{1}, \quad \forall \Gamma. \quad (\text{S23})$$

where we have denoted with  $H_{\text{G}}$  the gauge Hamiltonian and  $G_\Gamma$  the group of its gauge symmetries and by  $H_{\text{G}}$  the image (non-gauge) Hamiltonian.

A gauge-reducing duality needs to be implementable as a projective unitary operator  $\mathcal{U}$  only:

$$\Phi_{\text{GR}}(\mathcal{O}) = \mathcal{U} \mathcal{O} \mathcal{U}^\dagger, \quad \mathcal{U} \mathcal{U}^\dagger = \mathbb{1}, \quad \mathcal{U}^\dagger \mathcal{U} = P_{\text{GI}} \quad (\text{S24})$$

where  $P_{\text{GI}}$  is the projector of the subspace of gauge-invariant states, i.e.  $G_\Gamma |\psi\rangle = |\psi\rangle$  for all  $\Gamma$ .

A clear example of a gauge-reducing duality is provided by the  $\mathbb{Z}_N$  gauge model in two-dimensions of (S10), whose symmetry group is generated by (S3). For simplicity we illustrate here the  $\mathbb{Z}_2$  case, where the  $V$ ’s are taken to be the Pauli operators  $\sigma^z$  and the  $U$ ’s to be  $\sigma^x$ , so that the Gauss operators are given by

$$G_r = \sigma_{(x,\hat{1})}^z \sigma_{(x,\hat{2})}^z \sigma_{(x,-\hat{1})}^z \sigma_{(x,-\hat{2})}^z, \quad (\text{S25})$$

while the gauge-invariant bond algebra is generated by

$$\left\{ \sigma_{(x,\hat{1})}^z, \sigma_{(x,\hat{2})}^z, U_\square \right\} \quad (\text{S26})$$

for which the following relations hold:

- all the bonds square to the identity;
- each spin  $\sigma^z$  anti-commutes with two adjacent plaquettes operators  $U_\square$ ;

- each plaquette operator  $U_{\square}$  anti-commutes with four spins  $\sigma^z$ .

This set of relations is identical to those satisfied by the bonds of the two-dimensional quantum Ising model, whose Hamiltonian is

$$H_{\text{I2d}}(h) = - \sum_i \left( \sigma_{i-1}^z \sigma_i^z + \sigma_{i-2}^z \sigma_i^z \right) - h \sum_i \sigma_i^x, \quad (\text{S27})$$

where  $i$  runs over the sites of a suitable lattice, and to which we now construct a duality transformation  $\Phi_{\text{GR}}$ . In order to do so, we define the dual lattice of the model (S10) by identifying a site  $i$  of the dual lattice with the plaquette  $\square$  having the site  $x$  in the lower-left corner. Then, we set:

$$\begin{aligned} \Phi_{\text{GR}} \left( \sigma_{(x,\hat{1})}^z \right) &= \sigma_{i-2}^z \sigma_i^z, \\ \Phi_{\text{GR}} \left( \sigma_{(x,\hat{2})}^z \right) &= \sigma_{i-1}^z \sigma_i^z, \\ \Phi_{\text{GR}}(U_{\square}) &= \sigma_i^x. \end{aligned} \quad (\text{S28})$$

These equations are expressing the fact that physical states of the gauge model can be described entirely by the magnetic states of the plaquettes and that, in an Abelian gauge theory, the local gauge constraints impose the state of electric field on a given link to be the result of the difference between the adjacent plaquettes, i.e. to describe the domain wall between the plaquettes. Finally, making use of some simple algebra one can show that the Hamiltonian (S10) for  $N = 2$  is mapped into the two-dimensional Ising model with  $h = 1/\lambda$

$$\Phi_{\text{GR}}(H_{\mathbb{Z}_2}(\lambda)) = \lambda H_{\text{I2d}}(1/\lambda) \quad (\text{S29})$$

and that  $\Phi(G_r) = \mathbb{1}$ .

These considerations can be easily generalized to the Hamiltonian with the  $\mathbb{Z}_N$  symmetry, which is mapped onto an  $N$ -clock model [47].

### III. DUALITY BETWEEN LADDER LGT AND CLOCK MODELS

In this section we show how to construct a mapping of the  $\mathbb{Z}_N$  ladder LGT onto a  $N$ -clock model on a chain with a transversal field and a longitudinal field, the latter depending on the topological sector of the ladder LGT.

We start from the Hamiltonian (S10) written for a ladder geometry:

$$H_{\text{lad}}(\lambda) = - \sum_i \left[ U_i + \lambda \left( V_i^{\uparrow} + V_i^{\downarrow} + V_i^0 \right) + \text{h.c.} \right], \quad (\text{S30})$$

where we adopted the notation of the main text for the ladder.

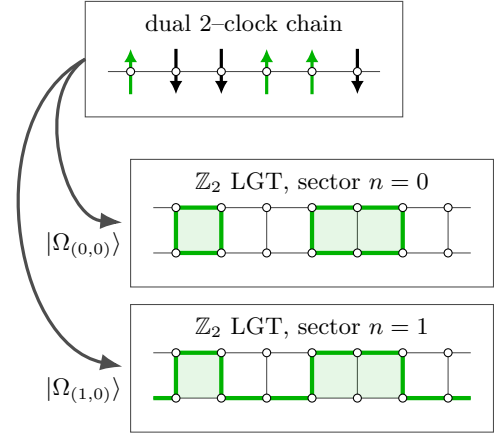


FIG. S4. Duality between the states of a 2-chain and the states of a  $\mathbb{Z}_2$  ladder LGT in the different sectors  $(0,0)$  ( $n = 0$ , no non-contractible electric loop) and  $(1,0)$  ( $n = 1$ , one non-contractible loop around the ladder). In the sector  $(0,0)$  it is evident that all the physical states contain closed electric loops. On the other hand, in the sector  $(1,0)$  the physical states are all the possible deformations of the electric string that goes around the ladder.

The duality of the previous section for two-dimensional gauge theories cannot be straightforwardly applied because here the links  $\ell^0$  have a different role when compared with the links  $\ell^{\uparrow}$  and  $\ell^{\downarrow}$ , only the former being *domain walls* between two plaquettes. Also, the electric operators  $V^{\downarrow}/V^{\uparrow}$  on the top/bottom links  $\ell^{\uparrow}/\ell^{\downarrow}$  have to be treated separately because they have different commutation relations with the plaquette operators  $U_i \equiv U_i^{\downarrow} U_{i+1}^0 (U_i^{\uparrow})^{\dagger} (U_i^0)^{\dagger}$ :

$$U_i V_i^{\downarrow} = \omega V_i^{\downarrow} U_i, \quad U_i V_i^{\uparrow} = \omega^{-1} V_i^{\uparrow} U_i. \quad (\text{S31})$$

Moreover, on a ladder the local Gauss operators get modified due to the fact that only three-legged vertices exist. They read as: The Gauss operators on the top and bottom vertices on the ladder become respectively

$$G_i^{\uparrow} = V_i^{\uparrow} (V_{i-1}^{\uparrow})^{\dagger} (V_i^0)^{\dagger}, \quad G_i^{\downarrow} = V_i^{\downarrow} V_i^0 (V_{i-1}^{\downarrow})^{\dagger}. \quad (\text{S32})$$

The duality transformation is defined through the following steps. First, the electric field on a vertical link  $\ell^0$  is mapped to  $Z_{i-1}^{\dagger} Z_i$ , as it is the result of the difference of the magnetic states of the two adjacent plaquettes. This can be readily verified, since from the definition of the plaquette operator  $U_i$  we get

$$V_i^0 U_i = \omega^{-1} U_i V_i^0, \quad V_i^0 U_{i-1} = \omega U_{i-1} V_i^0,$$

therefore the maps

$$U_i \mapsto X_i, \quad V_i^0 \mapsto Z_{i-1}^{\dagger} Z_i, \quad (\text{S33})$$

conserve the commutation relations of  $U_i$  and  $V_i^0$ . Notice that, since from (S32) we have

$$\prod_i G_i^{\downarrow} |\psi_{\text{phys}}\rangle = \prod_i V_i^0 |\psi_{\text{phys}}\rangle = |\psi_{\text{phys}}\rangle, \quad (\text{S34})$$

we expect that after the duality, the product of all  $V_i^0$  is mapped to the identity, as it is from (S33). This works as a sanity check for the duality map.

Second, we consider  $V^\uparrow$  and  $V^\downarrow$ , that commute with  $V^0$  while satisfy relations (S31) with respect to  $U_i$ . This allows us to assume:

$$V_i^\downarrow \mapsto c_i^\downarrow Z_i, \quad V_i^\uparrow \mapsto c_i^\uparrow Z_i^\dagger, \quad (\text{S35})$$

where  $c_i^\downarrow$  and  $c_i^\uparrow$  are complex numbers, with  $|c_i^\downarrow| = |c_i^\uparrow| = 1$  to guarantee unitarity. To further constraint the value of these coefficients, we can impose that the Gauss constraints (S32) has to become the identity:  $G_i^\uparrow \mapsto \mathbb{1}$  and  $G_i^\downarrow \mapsto \mathbb{1}$  for all  $i$ . Since:

$$\begin{aligned} G_i^\uparrow &\mapsto (c_i^\uparrow Z_i^\dagger)(c_{i-1}^\uparrow Z_{i-1}^\dagger)(Z_i^\dagger Z_{i-1})^\dagger = c_i^\uparrow (c_{i-1}^\uparrow)^*, \\ G_i^\downarrow &\mapsto (c_i^\downarrow Z_i)(Z_i^\dagger Z_{i-1})(c_{i-1}^\downarrow Z_{i-1}^\dagger) = c_i^\downarrow (c_{i-1}^\downarrow)^* \end{aligned} \quad (\text{S36})$$

we easily find that [48]:

$$c_i^\downarrow = c^\downarrow, \quad c_i^\uparrow = c^\uparrow, \quad \forall i. \quad (\text{S37})$$

Finally, we notice that superselection sectors are identified by the eigenvalue of the operator  $\bar{S}_2$  in (S13), which in the ladder geometry becomes

$$\bar{S}_2 = V_{i_0}^\uparrow V_{i_0}^\downarrow \quad (\text{S38})$$

for any fixed  $i_0$ , whose eigenvalue are simply  $\omega^k$ , for  $k = 0, \dots, N-1$ . Therefore using the mapping (S35) on (S38) in the sector with eigenvalue  $\omega^k$ , we get

$$\bar{S}_2 \mapsto (c^\uparrow Z_i^\dagger)(c^\downarrow Z_i) = c^\uparrow c^\downarrow = \omega^k. \quad (\text{S39})$$

This allows us to fix these coefficients as follows:

$$c^\uparrow = 1, \quad c^\downarrow = \omega^k. \quad (\text{S40})$$

In summary, the duality mapping for the topological sector  $\omega^k$  of the  $\mathbb{Z}_N$  LGT on a ladder reads as:

$$\begin{aligned} U_i &\mapsto X_i, & V_i^0 &\mapsto Z_{i-1}^\dagger Z_i, \\ V_i^\uparrow &\mapsto Z_i^\dagger, & V_i^\downarrow &\mapsto \omega^k Z_i. \end{aligned} \quad (\text{S41})$$

The transformed Hamiltonian is:

$$H_{\text{lad}}(\lambda) \mapsto \lambda H_N(\lambda^{-1}) \quad (\text{S42})$$

where

$$H_N(\lambda^{-1}) = - \sum_i \left( Z_{i-1}^\dagger Z_i + \frac{1}{\lambda} X_i + (1 + \omega^k) Z_i + \text{h.c.} \right) \quad (\text{S43})$$

i.e. a clock model with both *transversal* and *longitudinal* fields, where the value of the latter carries the information of the superselection sector.

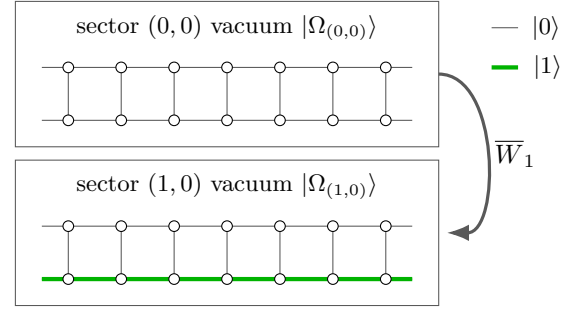


FIG. S5. The different “Fock vacua”  $|\Omega_{(0,0)}\rangle$  and  $|\Omega_{(1,0)}\rangle$  of the  $\mathbb{Z}_2$  ladder LGT. The latter can be obtained from the former by applying the Wilson loop operator  $W_1$ . The states  $|0\rangle$  and  $|1\rangle$  refer to the eigenstates of the electric field operator  $V$ , which is just  $\sigma_z$  in the  $\mathbb{Z}_2$  model.

#### IV. IMPLEMENTATION OF THE GAUSS LAW

When considering a LGT, one would like to work within the physical subspace, which is obtained by imposing Gauss law at every site. A “brute-force” method, in which one generates all the possible states and then filters out all the states that violate Gauss law, is clearly not efficient, even for moderately small lattices. To better exemplify this, consider a  $\mathbb{Z}_2$  theory on a  $L \times L$  periodic lattice, which have  $L^2$  sites and  $2L^2$  links, and only  $2^{L^2}$  physical states. There are therefore  $2^{2L^2}$  possible states and for each one up to  $L^2$  checks (one per site) has to be performed. As a result, the construction of the physical Hilbert space involves  $O(L^2 2^{2L^2})$  operations in a search space of  $2^{2L^2}$  objects for finding only  $2^{L^2}$  elements. In this work, we exploit the gauge-reducing duality map described in Sec. II and III to devise an algorithmic procedure that generates physical configurations starting from the states of the dual clock model. This is not a search or pattern-matching algorithm and gives a *major speedup* with respect to the brute-force method.

Given a  $\mathbb{Z}_N$  LGT on a lattice of size  $L \times L$ , we consider the dual  $N$ -clock model on a similar lattice with  $A = L^2$  sites. A basis for the Hilbert space of the clock-model is the set of states  $|\{s_i\}\rangle \equiv |s_0 s_1 \dots s_{A-1}\rangle$ , with  $s_i = 0, \dots, N-1$ . The corresponding gauge-invariant state in each superselection sector  $\mathcal{H}_{\text{phys}}^{(n,m)}$  of the Hilbert space of the dual LGT model is given by:

$$|\{s_i\}\rangle \mapsto \prod_{i=0}^{A-1} U_i^{s_i} |\Omega_{(n,m)}\rangle, \quad (\text{S44})$$

where  $U_i$  is the plaquette operator on the  $i$ -th plaquette and  $|\Omega_{(n,m)}\rangle$  is the “Fock vacuum” of the  $\mathcal{H}_{\text{phys}}^{(n,m)}$  subspace. Moreover, the “Fock vacuums”  $|\Omega_{(n,m)}\rangle$  can be obtained easily, thanks to (S17):

$$|\Omega_{(n,m)}\rangle = (\bar{W}_1)^n (\bar{W}_2)^m |\Omega_{(0,0)}\rangle, \quad (\text{S45})$$

where  $|\Omega_{(0,0)}\rangle$  is the vacuum in the  $(0,0)$ -sector, i.e. the state  $|000\cdots 0\rangle$ . Fig. S4 and S5 show some examples.

Let us quantify the obtained speedup with this method. In the case of a  $\mathbb{Z}_2$  theory on a square lattice  $L \times L$  there are  $2^{L^2}$  possible clock configurations. For each configuration, there are at most  $L^2$  magnetic fluxes to apply. This translates into  $O(L^2 2^{L^2})$  operations: notice that the exponent does not contain the factor 2 which is present in the “brute-force” method, thus reducing the number of operations by an order of  $O(2^{L^2})$ .

This procedure is easily generalizable for any  $\mathbb{Z}_N$ .

## V. DISTRIBUTION OF THE AMPLITUDES IN THE GROUND STATE

In the  $N = 2$  case, we further differentiate the phase diagrams of the two sectors by looking at the ground state amplitudes distribution, for  $\lambda < 1$  and  $\lambda > 1$ . Obviously, the ground state can be written as a superposition of the gauge invariant states of  $\mathcal{H}_{\text{phys}}$  in the given sector

$$|\Psi_{\text{g.s.}}\rangle = \sum_n c_n |n\rangle. \quad (\text{S46})$$

The basis  $|n\rangle$  and the amplitudes  $c_n$  are sorted in a decreasing order with respect to the modulus of the latter. The first state of the list, with amplitude  $c_1$ , is always the Fock vacua  $|\Omega\rangle$  of the sector, hence we consider the distribution of the ratios  $|c_n/c_1|$ , which are plotted in Fig. S7–S6 for  $\lambda = 0.1$  and  $\lambda = 1.5$ , respectively. The most interesting one is at  $\lambda = 0.1$ , where the difference between the deconfined phase in the sector  $(1,0)$  and the confined one in the sector  $(0,0)$  can be seen. In particular, in the deconfined phase the ground state is a superposition of deformations of the Fock vacuum, i.e. the non-contractible electric string, which can be thought as a *kink condensate* [34] (or as a paramagnetic phase), where each kink corresponds to a deformation of the string. Meanwhile, for  $\lambda > 1$ , where we have confinement in both sectors, the ground state is essentially a product state, akin to a ferromagnetic state. This is explained in Fig. S7 and Fig. S6.

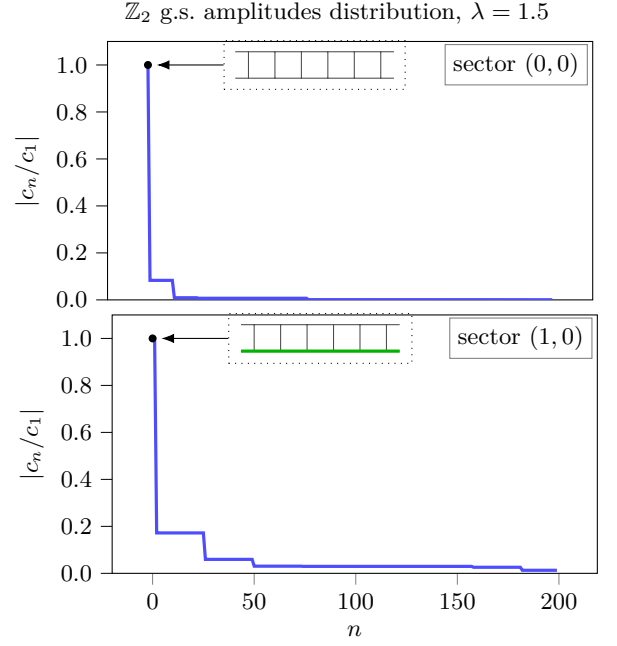


FIG. S6.  $\mathbb{Z}_2$  ground state amplitude distribution for  $\lambda = 1.5$  of the first 200 states and with lattice size  $12 \times 2$ . For both sectors  $(0,0)$  (top) and  $(1,0)$  (bottom) we are in a confined phase, which corresponds to a ferromagnetic phase in the Ising chain. Here we see a polarized state where the domain walls are suppressed and the ground state is essentially a product state.



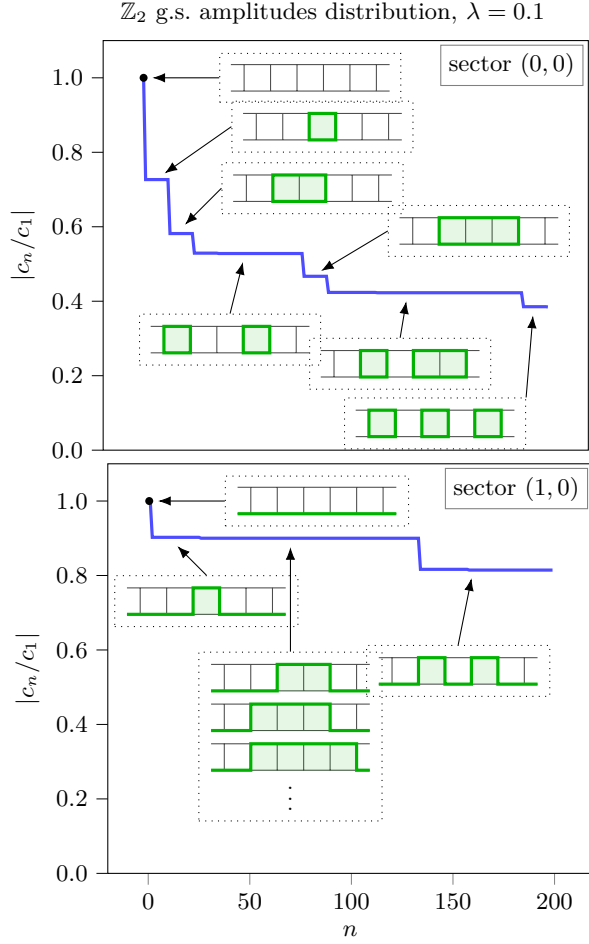


FIG. S7.  $\mathbb{Z}_2$  ground state amplitude distribution for  $\lambda = 0.1$  of the first 200 states and with lattice size  $12 \times 2$ . *Top*: distribution of the ratios  $|c_n/c_1|$  for the sector  $(0,0)$  (see (S46)). We see that the heaviest states that enter the ground state, apart from the vacuum that sets the scale, are made of small electric loops, typical of a confined phase. *Bottom*: the same distribution of ratios for the sector  $(1,0)$ . We see that the heaviest states are made of bigger and bigger deformations of the electric string that goes around the ladder. This happens because the energy contributions depend only on the domain walls between two plaquettes with different flux content. This behaviour is similar to the so-called *kink condensation* in spin chains [34], where the disordered state can be expressed as a superposition of all possible configuration of kinks (i.e. domain walls between two differently ordered regions). In the language of the duality, this deconfined phase then maps to the paramagnetic phase of the quantum Ising model with *only* transverse field.